J. Biomed. Eng. Res.
Vol. 20, No 6, 523-529, 1999

Implementing a Fast Projector-Backprojector for EM-Based Tomographic Reconstruction

S.J. Lee

Department of Electronic Engineering, Paichai University

(Received July 12, 1999, Accepted November 13, 1999)

요 약 : 방출컴퓨터단층영상술을 위한 영상재구성법에 있어서 기대값 최대화(EM)를 사용한 maximum likelihood 방법이 기존의 filtered backprojection 방법에 비해 현저한 장점을 지니고 있다는 점에서 지속적으로 그 가치가 인정되어 왔다. 그러나, 이러한 방법은 projection 및 backprojection의 반복계산을 요하므로 영상재구성을 위한 총 계산시간이 projector 및 backprojector의 성능에 크게 좌우된다. 본 논문에서는 EM에 근거한 영상재구성 알고리즘의 계산량을 감소시키는 방법에 관하여 논한다. 특히 projection 및 backprojection 계산을 위한 행렬의 원소 중 중요한 양들을 구하는 방법과 이들을 미리 계산하여 적절한 양의 메모리에 저장하는 방법에 관하여 고찰한다. 실험에서 제안된 방법을 사용할 경우 표준 EM 알고리즘의 계산시간을 92% 까지 현저히 감소시킬 수 있음을 보였다.

Abstract : Iterative reconstruction methods based on the maximum likelihood approach using the expectation maximization (EM) algorithm have enjoyed continuing interest in emission computed tomography due to their remarkable advantages over the conventional filtered backprojection method. However, since these methods require the calculation of projection and backprojection for every iteration, the total computer time for reconstructing an image highly depends on the performance of the projector-backprojector implemented in an algorithm. In this paper, we discuss techniques for reducing the computational requirements of the EM-based reconstruction algorithms. Specifically, the paper discusses methods of generating important quantities of the matrix used for forward and backprojection and precomputing them to fit into a moderate amount of computer memory. Our experimental results show that the proposed method dramatically reduces CPU time up to 92% for the standard EM algorithm

Key words : Emission computed tomography, Image reconstruction from projections, Expectation maximization

INTRODUCTION

Emission computed tomography (ECT), such as single-photon emission computed tomography (SPECT) or positron emission tomography (PET), has played a prominent role in the area of nuclear medicine by providing functional information about physiological processes in the human body. The objective of ECT is to determine the three dimensional (3-D) distribution of radionuclide concentrations within the body using 2-D projectional views acquired at many different angles about the patient. Therefore, the reconstruction problem in ECT is to compute the distribution of a radionuclide in a given cross section of the human body from the projection measurements. Unfortunately, since the observed data in ECT systems are contaminated by noise due to low count rate and physical factors such as attenuation, scatter, and detector response, it has been a difficult problem to reconstruct images with good accuracy.

Recently, the application of the maximum likelihood (ML) approach using the expectation maximization algorithm [1] has enjoyed continuing interest in ECT since they can in principle naturally express accurate system models of physical effects, and can accurately model the statistical character of the data. The ML-EM approach has also led to the introduction of extended approaches, such as a variety of important Bayesian adaptions of EM [2-5]. Despite the several advantages of ML-EM and other Bayesian approaches including our own early work [4,5], EM-based algorithms suffer from a slow rate of convergence due to the high iteration numbers to achieve an acceptable image. To overcome this problem, recent papers have emphasized the acceleration of the EM algorithm either by using the geometry of the system [6] or by developing block iterative

본 논문은 보건복지부 '98보건의료기술연구개발사업(과제번호: HMP-98-E-1-0008) 지원으로 이루어졌음.

통신저자 : 이수진, (302-735) 대전시 서구 도마 2동 439-6
배재대학교 전자공학과
Tel. (042)520-5711, Fax. (042)520-5663
E-mail. sjlee@mail.paichai.ac.kr

algorithms [7 9]. Kaufman [6] showed that, for PET reconstruction, the cost of each iteration can be reduced by using a "ring" grid instead of the traditional square grid since the ring grid takes advantage of the rotational symmetry of the system. In this case, however, a vague outline of the circular sectors may appear in the reconstructed image [6]. On the other hand, block iterative algorithms can accelerate convergence by sequentially processing blocks of projections and do not require additional modification of the geometric structure. However, these approaches still require several iterations to converge to a good solution. In all cases, the EM-based algorithms require repeated calculations of projection and backprojection.

In this paper, we propose an improved method for implementing a fast projector-backprojector, which can significantly accelerate EM-based reconstruction algorithms including block iterative algorithms. The remainder of this paper describes the overview of the EM algorithm, develops our fast projector-backprojector along with its implementational details, and presents simulation results showing a significantly improved performance in CPU time.

THE EM ALGORITHM FOR EMISSION TOMOGRAPHY

In ECT a radiopharmaceutical containing a radioactive isotope is introduced into the body and forms an unknown emitter (source) density (or distribution). A dominant source of degradation in ECT is photon noise due to fluctuations in the number of photons emitted from the underlying object. For a two-dimensional (2-D) distribution of underlying source f_{ij} on a single cross-sectional plane, we define $g_{t\theta}$ as the number of detected counts in the detector bin indexed by t at angle θ. Since the number of detected counts in ECT is independently Poisson distributed, the EM algorithm is derived from the likelihood probability distribution, which is given by

$$\Pr(g|f) = \prod_{t\theta} \frac{\bar{g}^{g_{t\theta}} \exp(-\bar{g}_{t\theta})}{g_{t\theta}!}, \tag{1}$$

where $\bar{g}_{t\theta}$ is the expected number of counts and is defined as $\bar{g}_{t\theta} = \sum_{ij} H_{t\theta,ij} f_{ij}$. Here, $H_{t\theta,ij}$ is the probability that a photon emitted from source location (i,j) hits detector bin t at angle θ. A matrix $\boldsymbol{H}$, whose elements are specified by $H_{t\theta,ij}$, is then the "system matrix" since it summarizes all of the knowledge on the physical process of emission of a photon to its detection. The implementational details on the $\boldsymbol{H}$ matrix are described in the following section.

One possible solution to the reconstruction problem is to maximize the likelihood given in (1). The maximum likelihood estimate (MLE) attempts to find the object $\hat{f}$ that is most likely to have given rise to the collected data g. Mathematically, the solution for the MLE can be expressed as

$$\hat{f} = \arg\max_{f} \Pr(g|f)$$

The EM algorithm proposed in [1,10] is an iterative algorithm that produces a sequence of estimates of f that converges to the MLE. The objective function for EM is given by

$$Q(f|\hat{f}) = \sum_{t\theta}\sum_{ij}\left[g_{t\theta} \frac{H_{t\theta,ij}\hat{f}_{ij}}{\sum_{kl} H_{t\theta,kl}\hat{f}_{kl}} \log(f_{ij}) - H_{t\theta,ij} f_{ij} \right]. \tag{2}$$

Taking partial derivatives, setting them equal to zero, and solving for f_{ij} results in an update equation for the EM algorithm:

$$\hat{f}_{ij}^{n+1} = \frac{\hat{f}_{ij}^{n}}{\sum_{t\theta} H_{t\theta,ij}} \cdot \sum_{t\theta} \frac{g_{t\theta} H_{t\theta,ij}}{\sum_{kl} H_{t\theta,kl}\hat{f}_{kl}^{n}}, \tag{3}$$

where $\hat{f}_{ij}^{n+1}$ and $\hat{f}_{ij}^{n}$ in (3) are f_{ij} and $\hat{f}_{ij}$ in (2), respectively. Note that $g_{t\theta}$ and $\sum_{kl} H_{t\theta,kl}\hat{f}_{kl}^{n}$ in (3) are the observed projection measurements and the mean of estimated counts, respectively. By defining $\hat{\bar{g}}_{t\theta}^{n} = \sum_{ij} H_{t\theta,ij}\hat{f}_{ij}^{n}$, we may rewrite the update equation as

$$\hat{f}_{ij}^{n+1} = \frac{\hat{f}_{ij}^{n}}{\sum_{t\theta} H_{t\theta,ij}} \cdot \sum_{t\theta}\left\{ H_{t\theta,ij} \frac{g_{t\theta}}{\hat{\bar{g}}_{t\theta}^{n}} \right\} \tag{4}$$

Notice that the second term ($\sum_{t\theta}\{\}$) on the right side of (4) is the "backprojection" of $g_{t\theta}/\hat{\bar{g}}_{t\theta}^{n}$. Therefore, the EM algorithm is implemented by iterations requiring projection and backprojection calculations. Starting with some initial estimate $\hat{f}^{0} > 0$, the EM algorithm consists of the following steps:

SET $n := 0$;

REPEAT until convergence of $\hat{f}^n$

(i) PROJECT $\hat{f}^n$ to calculate the mean values for cumulated counts $g_{t\theta}$:

$\hat{g}_{t\theta}^{\,n} := \sum_{ij} H_{t\theta,ij}\ \hat{f}_{ij}^{\,n}$;

(ii) BACKPROJECT $g_{t\theta} / \hat{g}_{t\theta}^{\,n}$ to calculate

$\sum_{t\theta}\left\{ H_{t\theta,ij} \frac{g_{t\theta}}{\hat{g}_{t\theta}^{\,n}} \right\}$;

(iii) UPDATE pixels $\hat{f}^{n+1}$ using (4);

(iv) $n := n+1$;

END

Notice that, since the EM algorithm requires projection and backprojection for every iteration, computer time highly depends on the performance of the projector backprojector implemented in the algorithm.

Hudson and Larkin [7] proposed an accelerated version of the EM algorithm, the ordered subsets (OS) algorithm, that processes the data in blocks (subsets) within each iteration. In their work, they showed that the procedure accelerated convergence by a factor proportional to the number of blocks. Unfortunately, however, the closeness to the likelihood in the OS-EM algorithm is known to be inversely proportional to the number of blocks. Therefore, the OS EM algorithm with reasonable number of blocks still requires several iterations to achieve the closeness to the likelihood .

IMPLEMENTING A FAST PROJECTOR-BACKPROJECTOR

As described in the previous section, the system matrix contains weight factors for the forward projection based on the system characteristics. Each weight factor represents the probability that a photon emitted from a certain source position in f will be detected at a certain position of the detector in g. In theory, $\boldsymbol{H}$ can be obtained by placing a point source at each location in f and by measuring the response at each of the detectors in g. In this case the size of the matrix $\boldsymbol{H}$ would be extremely large. In practice, however, $\boldsymbol{H}$ is implicitly computed based on the source-detector geometry, and the physical processes are adequately modeled as linear effects.

As shown in Fig. 1, if a given ray is indexed by (t, θ) and a pixel located at (i, j) is passed by the projection ray,

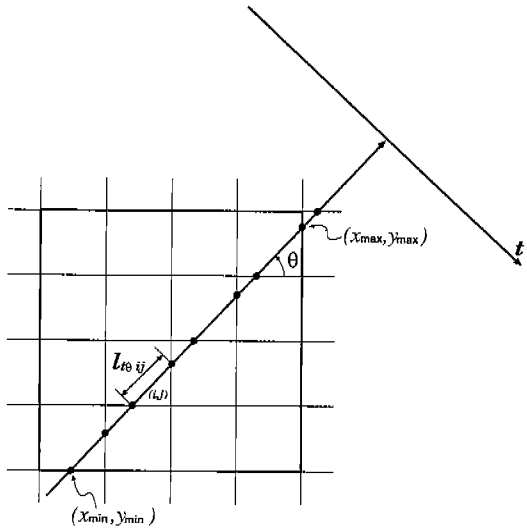

Fig. 1. Geometry for calculation of quantities in Siddon's method

some photons emitted from this pixel will be detected at detector bin (t, θ) since it is viewed by the collimator. Let $l_{t\theta,ij}$ be the intersecting length of the ray indexed by (t, θ) through the pixel located at (i, j). Then the longer the length, the more counts it will be received by the detector. Hence an approximation of each element of the system matrix may be $H_{t\theta,ij} \doteq l_{t\theta,ij}$.

Although very simple in principle, the exact evaluation of the intersecting length has proven to be a time consuming and difficult problem. To accelerate the calculation of the exact intersecting length $l_{t\theta,ij}$, Siddon [11] proposed an efficient way of calculating the intersecting length by considering the pixels as the intersection areas of orthogonal sets of equally spaced, parallel lines as shown in Fig. 1. In this case, instead of calculating the intersections of the ray with the individual pixels, the intersections of the ray with the *lines* are calculated. This is apparently more efficient and simpler than calculating the intersections of the ray with the individual pixels in that, as the lines are equally spaced, it is only necessary to determine the first intersection and generate all the others by recursion. Using the two intersection points of the ray with the sides, (x_{min}, y_{min}) and (x_{max}, y_{max}), the Siddon's method provides (i) the number of pixels N that the ray passes through, (ii) the length of the ray contained by each pixel (in units of the ray length), and (iii) the corresponding pixel indices (i, j).

For SPECT reconstruction, it is necessary to calculate the exact intersecting length $l_{t\theta,ij}$ in order to correct the effect of attenuation. Liang *et al.* [12] utilized the Siddon's

method to recursively compute attenuation factors along each projection ray starting at the pixel closest to the detector. (The details on modeling other factors in SPECT, such as scatter and detector response, can also be found in [12].) Let a given ray be indexed by (t, θ). The 2 D coordinates of the nth pixel along that ray, a quantity computed by the Siddon's method, is then denoted $(i_{t\theta}(n), j_{t\theta}(n))$, with $n=1$ denoting the pixel closest to the detector. For each pixel, an attenuation factor, $A(i_{t\theta}(n), j_{t\theta}(n))$, is computed by adding half of the attenuating length in the pixel and the previously accumulated attenuating length along the projection ray:

$$A(i_{t\theta}(n), j_{t\theta}(n)) = \exp\Big[-\sum_{k=1}^{n-1}\mu(i_{t\theta}(k), j_{t\theta}(k))\, l_{t\theta}(k) - \frac{1}{2}\mu(i_{t\theta}(n), j_{t\theta}(n))\, l_{t\theta}(n)\Big], \tag{5}$$

where $\mu(i_{t\theta}(n), j_{t\theta}(n))$ and $l_{t\theta}(n)$ are the average attenuation coefficient and the intersecting length of the nth pixel in the ray indexed by (t, θ), respectively. Having computed the attenuation factor, the forward projection $g_{t\theta}$ may be written as

$$g_{t\theta} = \sum_{n=1}^{N} A(i_{t\theta}(n), j_{t\theta}(n))\, l_{t\theta}(n),$$

where N is the number of pixels in the ray indexed by (t, θ). Note that, for $\mu(\cdot)=0$, which is the case for no attenuation media, the forward projection reduces to .

$$g_{t\theta} = \sum_{n=1}^{N} l_{t\theta}(n)$$

Though Siddon's method provides an efficient way to calculate the intersecting lengths along the ray, it is no longer efficient if it is repeated for every iteration within the EM algorithm. To avoid the repeated calculations of the intersecting lengths, we propose a more efficient way of using the Siddon's quantities by storing the intersecting lengths $l_{t\theta}(n)$ or the attenuating lengths $(l(n)\ A(i_{t\theta}(n), j_{t\theta}(n)))$ for attenuation correction and the corresponding detector bin t in look up tables during the forward projection before the first iteration of the algorithm. Each element in the tables is addressed by the pixel location (i, j) and the angle θ. In other words, for a given ray toward (t, θ), the attenuation length and the index t are stored in $(i(n), j(n), \theta)$ of the tables. Since multiple rays can pass through a pixel, the maximum value for the number of rays passing through a pixel should be determined from the source detector geometry of a given system. In this paper, we assume that the maximal number of rays passing through a pixel is two, which is reasonable for most conventional ECT systems. In this case two pairs of arrays are needed to specify the two rays. Let $t_1(i(n), j(n), \theta)$ and $attlen_1(i(n), j(n), \theta)$ be the 3 D arrays for storing the index t and the attenuation length obtained from the first ray passing through a pixel located at $(i(n), j(n))$, respectively, where n is the pixel index obtained from the Siddon's method. Similarly, another pair of the arrays, $t_2(i(n), j(n), \theta)$ and $attlen_2(i(n), j(n), \theta)$ are for the second ray passing through the pixel. For K angles and L detector bins, the procedure to store the Siddon's quantities is then summarized as follows:

```
set t1(·): = 0; t2(·): =0;
set attlen1(·): = 0; attlen2(·): =0;
for θ =1, 2, ···, K
    for t =1, 2, ···, L
        calculate (x_min, y_min) and (x_max, y_max);
        compute Siddon's quantities,
         N≡n, (i(n),j(n)), and l(n);
        for n=1, 2,···, N
            compute attenuation length, attlen;
            store the index t and the attenuation
            length attlen using
            if( t1(i(n), j(n), θ) == 0 )
                t1(i(n), j(n), θ): =t;
                attlen1(i(n), j(n), θ): =attlen;
            else
                t2(i(n), j(n), θ): =t;
                attlen2(i(n), j(n), θ): =attlen;
            end if
        end
    end
end
```

Having stored the quantities obtained from the Siddon's method, projection for each angle can now be calculated by simply accumulating the attenuating lengths for each pixel obtained from the tables as shown below:

```
set g_tθ := 0 for ∀ t and θ;
for i=1, 2,···, M
    for j=1, 2,···, M
        for θ=1, 2,···, K
            t := t_1(i, j, θ);
            g_tθ := g_tθ + f_ij × attlen_1(i, j, θ);
            t := t_2(i, j, θ);
            g_tθ := g_tθ + f_ij × attlen_2(i, j, θ);
        end
    end
end
```

Since the above method does not involve the core steps of Siddon's method to calculate the intersecting lengths by tracing each projection ray, it significantly reduces computer time.

Let us now consider the backprojection step in (4). The conventional backprojection method is to smear the measurements back into the object domain. In this case it is necessary to calculate Siddon's quantities used in forward projection in order to distribute each measurement to pixels along the projection ray. However, it is again inefficient if the calculation of the Siddon's quantities for backprojection is repeated for every iteration.

One of the excellent features of using the quantities stored in the tables is that backprojection can be performed by pixel-by-pixel operations rather than conventional ray-by-ray operations, while retaining the advantages of using exact intersecting lengths. Let $b_{ij}=\sum_{t\theta}\left\{H_{t\theta,ij}\frac{g_{t\theta}}{\bar{\hat{g}}_{t\theta}^{\,n}}\right\}$, where $\bar{\hat{g}}_{t\theta}$ is calculated by projecting the reconstruction $\hat{f}_{ij}$ obtained from the previous iteration. The procedure for backprojection is then described as follows:

```
set b_ij := 0 for ∀ i and j;
for i=1, 2,···, M
    for j=1, 2,···, M
        for θ=1, 2,···, K
            t := t_1(i, j, θ);
            b_ij := b_ij + attlen_1(i, j, θ) × g_tθ / ĝ_tθ^n;
            t := t_2(i, j, θ);
            b_ij := b_ij + attlen_2(i, j, θ) × g_tθ / ĝ_tθ^n;
        end
    end
end
```

Note that, for $\frac{g_{t\theta}}{\bar{\hat{g}}_{t\theta}^{\,n}}=1$ in (4), the backprojection b_{ij} reduces to $b_{ij}=\sum_{t\theta}H_{t\theta,ij}$, which is the denominator of the first term in the right side of (4). This term is identified as the normalization which contains the relative total system sensitivity at each pixel (see Fig. 2 (d)). By inserting this term in the loop for θ in the above procedure, the entire EM algorithm can be readily implemented with a high efficiency for repeated calculations of projections and backprojections.

SIMULATIONS AND RESULTS

To test the performance of our projector-backprojector, we implemented the two EM-based reconstruction algorithms ;the standard EM proposed by Shepp and Vardi [1] and the OS-EM proposed by Hudson and Larkin [7]. For the OS-EM algorithm, we used two different numbers of subsets (8 and 16) to group the projection data. In fact, the standard EM algorithm is a special case of OS-EM whose number of subsets for all projection data is one. Therefore, the algorithms used in our simulations may be regarded as the OS-EM algorithms with a single subset, 8 subsets, and 16 subsets. To compare the CPU time for the EM-based algorithms implemented by using our fast projector-backprojector with those implemented by a conventional way, we also implemented a standard projector-backprojector that computes the intersecting lengths of each ray repeatedly using the Siddon's method at each iteration. Although our method can easily be extended to other EM-based algorithms, such as Bayesian MAP algorithms, only the results from the two algorithms are reported here because of the similarity of the results from MAP algorithms in terms of

Table 1. Comparison of CPU times for reconstructing a 128 × 128 image

	EM	OS-EM (8 blocks)	OSEM (16 blocks)
Number of iterations	64	8	4
CPU s for standard method (CPU s/iteration)	402.68 (6.29)	25.82 (3.24)	12.94 (3.24)
CPU s for proposed method (CPU s/iteration)	33.83 (0.47)	11.13 (0.92)	9.82 (1.47)
Reduction of total CPU s (%)	9.16	56.9	24.1

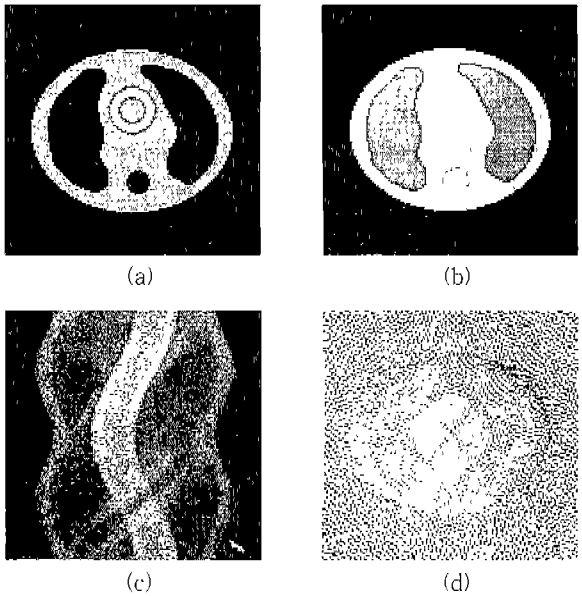

Fig. 2. The 128×128 phantom image used in the simulations and other reconstruction related images. (a) Chest phantom activity. (b) Attenuation map. (c) Sinogram with Poisson noise. (d) Surface plot for the sensitivity map obtained form (b)

computer time. The algorithms were programmed in GNU C (version 2.7) on the Linux operating system and run on a Pentium II processor running at 400 MHz.

The simulations were performed on a 2-D (128×128) elliptical chest phantom shown in Fig. 2(a). For projection data from the 128×128 phantom, we used 128 projection angles over 360° with 192 detector bins at each projection. Our reconstruction geometry was thus a 128×128 square image matrix with a detector array length slightly longer than the diagonal of the square. Figures 2 (a), (b), (c), and (d) show the chest phantom activity, the attenuation map, the simulated projection data (sinogram), and the sensitivity map obtained from the attenuation map, respectively. The chest phantom activity in myocardium, tissue, and lung was specified to be in the ratio 8:1:0. We assumed linear attenuation coefficients of 0 for air, 0.048 cm 1 for lung, 0.096 cm 1 for tissue, and 0.152 cm 1 for bone. Projection data were generated by incorporating attenuation and Poisson noise. In this case, the total number of detector counts in all projections was approximately 250,000.

For iteration numbers, we chose 64 for the standard EM, 8 for the OS-EM with 8 blocks, 4 for the OS-EM with 16 blocks. The number of iterations for the standard EM was chosen qualitatively based on the starting point for deterioration of the smoothness. The choices for the iteration numbers in OS-EM were made based on the fact that the OS-EM algorithm accelerates its convergence by a factor

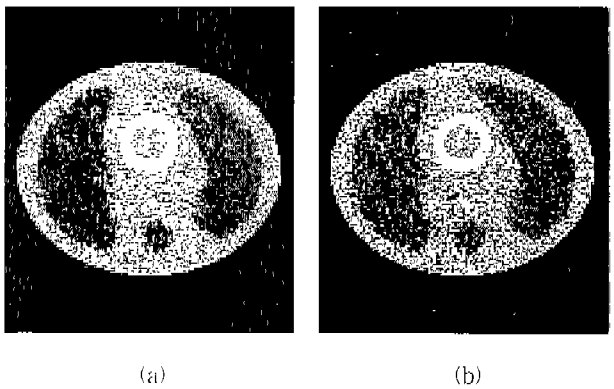

Fig. 3. Reconstructed images by ML-EM and OS-EM. (a) ML-EM(64 iterations). (b) OS-EM with 16 blocks(4 iterations)

proportional to the number of blocks [7]. Figures 3 (a) and (b) show the reconstructions by EM and OS-EM with 16 blocks, respectively.

Table 1 compares CPU seconds required to compute the update equation in (4) for 128×128 pixels. For standard EM, when our projector backprojector was used, the CPU time for 64 iterations was dramatically reduced from 402.68s to 33.83s.Note that our projector-backprojector requires only one-time calculation of the Siddon's quantities to be stored before the first iteration. The measured CPU time to calculate the Siddon's quantities and store them in computer memory was 3.96s and it was included in all CPU times for the proposed method in Table 1 except CPU s/iteration in (parentheses) for the proposed method. For OS-EM, while the improvement is not so stunning as the case for the standard EM, the CPU times for 8 (×8 blocks) iterations and 4 (×16 blocks) iterations were still significantly reduced from 25.82s to 11.13s and from 12.94s to 9.82s, respectively. Recall that the closeness of the solution obtained by OS EM to the likelihood is inversely proportional to the number of blocks used in the algorithm. Therefore, our projector backprojector implemented in an OS-EM algorithm allows less blocks to achieve a certain quality of solution in a given computer time. For example, as shown in Table 1, the OS-EM with 8 blocks implemented with our projector-backprojector is even faster than the OS-EM with 16 blocks implemented with the standard projector-backprojector (11.13 s vs. 12.94s).

The amount of memory required to store the Siddon's quantities in our projection geometry was approximately 20MB, where we used a single byte for both $t_1(\cdot)$ and $t_2(\cdot)$ and 4 byte floating point for both $attlen_1(\cdot)$ and $attlen_2(\cdot)$.

CONCLUSION

We have considered an improved method for implementing a fast projector backprojector, which is useful for iterative reconstruction algorithms that require repeated calculations of projection and backprojection, such as the ML EM and the EM-based Bayesian algorithms. An overall conclusion is that, by storing the intersections of the ray with the individual pixels in computer memory before the first iteration, the actual iterations can significantly be accelerated by simply using the quantities stored in the memory. Our experimental results show that our proposed method can reduce CPU time up to 92% for the standard EM algorithm. The OS EM algorithm, which requires much less iterations than the standard EM, can also be accelerated further by using our proposed method.

Since EM based reconstruction methods are inevitably necessary for clinical applications due to their remarkable advantages over the classical filtered backprojection method, our proposed method with parallel processing will make such reconstruction methods more practical.

REFERENCES

1. L. Shepp and Y. Vardi, "*Maximum Likelihood Reconstruction for Emission Tomography*", *IEEE Trans. Med. Imaging*, MI-1, pp. 113-122, 1982
2. T. Hebert and R. Leahy, "*A Generalized EM Algorithm for 3-D Bayesian Reconstruction for Poisson Data Using Gibbs Priors*", *IEEE Trans. Med. Imaging*, MI-8(2), pp. 194-202, 1989
3. P.J. Green, "*Bayesian Reconstructions from Emission Tomography Data Using a Modified EM Algorithm*", *IEEE Trans. Med. Imaging*, MI 9(1), pp. 84-93, 1990
4. S.J. Lee, A. Rangarajan, and G. Gindi, "*Bayesian Image Reconstruction in SPECT Using Higher Order Mechanical Models as Priors*", *IEEE Trans. Med. Imaging*, MI-14(4), pp. 669-680, 1995
5. S.J. Lee, I.T. Hsiao, and G.R. Gindi, "*The Thin Plate as a Regularizer in Bayesian SPECT Reconstruction*", *IEEE Trans. Nuclear Science*, NS-44(3), pp. 1381 1387, 1997
6. L. Kaufman, "*Implementing and Accelerating the EM Algorithm for Positron Emission Tomography*", *IEEE Trans. Med. Imaging*, MI-6, pp. 37-51, 1987
7. H.M. Hudson and R.S. Larkin, "*Accelerated Image Reconstruction Using Ordered Subsets of Porjection Data*", *IEEE Trans. Med. Imaging*, MI-13(4), pp. 601-609, 1994
8. A.R. De Pierro, "*A Modified Expectation Maximization Algorithm for Penalized Likelihood Estimation in Emission Tomography*", *IEEE Trans. Med. Imaging*, MI-14(2), pp. 132-137, 1995
9. J.A. Fessler, E.P. Ficaro, N.H. Clinthorne, and K. Lange, "*Grouped-Coordinate Ascent Algorithms for Penalized-Likelihood Transmission Image Reconstruction*", *IEEE Trans. Med. Imaging*, MI-16, pp. 166-175, 1997
10. K. Lange and R. Carson, "*EM Reconstruction Algorithms for Emission and Transmission Tomography*", *J. Comput. Assist. Tomogr.*, 8, pp. 306-316, 1984
11. R. Siddon, "*Fast Calculation of the Exact Radiological Path for a 3D CT Array*", *Med. Phys.*, 12, pp. 252-255, 1985
12. Z. Liang, T.G. Turkington, D.R. Gilland, R.J. Jaszczak, and R.E. Coleman "*Simultaneous Compensation for Attenuation, Scatter and Detector Response for SPECT Reconstruction in Three Dimensions*", *Phys. Med. Biol.*, 37, pp. 587-603, 1991